frontiers | Frontiers in Materials

TYPE Original Research
PUBLISHED 02 March 2023
DOI 10.3389/fmats.2023.1108717



OPEN ACCESS

EDITED BY
Mehran Khan,
Hong Kong Polytechnic University, Hong Kong SAR, China

REVIEWED BY
Peng Zhang,
Zhengzhou University, China
Muhammad Javed,
COMSATS Institute of Information Technology, Pakistan
Ahmed farouk Deifalla,
British University in Egypt, Egypt

*CORRESPONDENCE
Mohammad Arsalan Khan,
mohd.arsalan.khan@hotmail.co.uk
S. M. Anas,
mohdanas43@gmail.com
Mohammad Mursaleen,
mursaleenm@gmail.com

SPECIALTY SECTION
This article was submitted to Structural Materials, a section of the journal Frontiers in Materials

RECEIVED 26 November 2022
ACCEPTED 07 February 2023
PUBLISHED 02 March 2023

CITATION
Nikhade H, Birali RRL, Ansari K, Khan MA, Najm HM, Anas SM, Mursaleen M, Hasan MA and Islam S (2023), Behavior of geomaterial composite using sugar cane bagasse ash under compressive and flexural loading.
*Front. Mater.* 10:1108717.
doi: 10.3389/fmats.2023.1108717



# Behavior of geomaterial composite using sugar cane bagasse ash under compressive and flexural loading

Harshal Nikhade[1,2], Ram Rathan Lal Birali[1], Khalid Ansari[2], Mohammad Arsalan Khan[3,4]*, Hadee Mohammed Najm[3], S. M. Anas[5]*, Mohammad Mursaleen[6]*, Mohd Abul Hasan[7] and Saiful Islam[7]

[1]Department of Civil Engineering, Kavikulguru Institute of Technology and Science, Ramtek, India, [2]Department of Civil Engineering, Yeshwantrao Chavan College of Engineering, Nagpur, India, [3]Department of Civil Engineering, Zakir Husain College of Engineering and Technology, Aligarh Muslim University, Aligarh, India, [4]Geomechanics and Geotechnics Group, Kiel University, Kiel, Germany, [5]Department of Civil Engineering, Jamia Millia Islamia, New Delhi, India, [6]China Medical University Hospital, China Medical University (Taiwan), Taichung, Taiwan, [7]Civil Engineering Department, College of Engineering, King Khalid University, Abha, Saudi Arabia

The sugar industry produces a huge quantity of sugar cane bagasse ash in India. Dumping massive quantities of waste in a non-eco-friendly manner is a key concern for developing nations. The main focus of this study is the development of a sustainable geomaterial composite with higher strength capabilities (compressive and flexural). To develop this composite, sugarcane bagasse ash (SA), glass fiber (GF), and blast furnace slag (BF) are used. Ash generated from burning sugar cane in the sugar industry is known as sugar cane bagasse. To check the suitability of this secondary waste for use in civil engineering and to minimize risk to the environment in the development of sustainable growth, a sequence of compressive and flexural strength tests was performed on materials prepared using sugar cane bagasse ash (SA) reinforced by glass fiber (GF) in combination with blast furnace slag (BF) and cement (CEM). The effects of the mix ratios of glass fiber to bagasse ash (0.2%–1.2%), blast furnace slag to the weight of bagasse ash (10%), cement binding to bagasse ash (10%–20%), and water to sugar cane bagasse ash (55%) regarding the flexural strength, compressive strength, density, tangent modulus, stress–strain pattern, and load–deflection curve of the prepared materials were studied. According to the findings, compressive strength achieved a maximum strength of 1055.5 kPa and ranged from 120 to 1055.5 kPa, and the flexural strength achieved a maximum strength of 217 kPa and ranged from 80.1 to 217 kPa at different mix ratio percentages. The value of the initial tangent modulus for the cube specimens ranged between 96 and 636 MPa. For compression specimens with 20% cement, the density decreased from 1320.1 to 1265 kg/m$^3$, and the flexural strength decreased from 1318 to 1259.6 kg/m$^3$. With limitation in lower percentages of C/SA, the specimen cannot sustain its shape even after curing period. In comparing the previous research with the present experimental work, it was observed that the material proposed here is lightweight and can be utilised as a filler substance in weak compressible soils to improve their load-bearing capacity.

KEYWORDS

**glass fiber, bagasse ash, blast furnace slag, mechanical strength, sustainable geomaterial**

# 1 Introduction

The most common building material used globally is cement. Cement production is influenced by a nation's level of industrialization and modernization (Stafford et al., 2016). However, it generates a significant amount of carbon dioxide, almost 8% of the world's total, production, and for manufacturing purposes, it uses a lot of resources, including raw materials and energy (Anjos et al., 2020). As a result, academics are interested in long-term research on the cement industry to utilize various agricultures wastes and create cement-based sustainable materials (Talero et al., 2007; Rubenstein, 2012; Saleh et al., 2020) without compromising cement's durability, cost, or mechanical strength. It is possible to cut carbon dioxide emissions by up to 40%–50% (Cordeiro and Kurtis, 2017; Martirena and Monzó, 2018). Various common supplemental cementitious materials, such as blast furnace slag, fly ash, metakaolin, and natural pozzolans, have been used to lower the clinker-to-cement ratio (Bahurudeen et al., 2015; Cordeiro et al., 2018; Rajasekar et al., 2018). Recent research has looked at pozzolanic geomaterials, such as industrial and agricultural wastes (Cordeiro et al., 2011; Cordeiro et al., 2016; Andreão et al., 2019).

Cementitious compounds can be improved by using blast furnace slag and pozzolanic materials to combine their distinct physical and chemical properties (Khan et al., 2021). A secondary surface for hydrate precipitation and nucleation is provided by blast furnace slag (Bentz et al., 2017); however, the dilution effect (Rodríguez de Sensale and Rodríguez Viacava, 2018) can reduce the mechanical strength of this material, making it operate like a quasi-inert material at a high concentration (Bahurudeen and Santhanam, 2015). For the cement industry, the mixture of blast furnace slag and pozzolan is a desirable alternative. Since pozzolan can improve mechanical performance at advanced ages (Cordeiro et al., 2018).

Bagasse is the fibrous byproduct that remains after the sugarcane juice has been extracted (Deepika et al., 2017). Sugarcane businesses produce sugarcane bagasse ash (SA) as a byproduct of the auto-combustion procedure in cogeneration boilers (Rao et al., 2021) as shown in Figure 1. Bagasse was first primarily utilized in the manufacture of paper (Kuruba et al., 2020). Due to its sufficient calorific content, bagasse is used as a fuel feedstock in the cogeneration boilers of the sugar industry to produce electricity (Bartošek, 2014). Nearly all of the sugar facilities in India and other nations that produce sugar have quickly built cogeneration systems due to the significant money generation connected to this process (Bartošek, 2014). Bagasse is a suitable feedstock for cogeneration boilers; however, disposing of the leftover ash causes serious environmental issues (Rodrigues, 2011). The discharge of bagasse ash causes serious contamination to nearby water bodies and land because of the light unburned fibre debris that is present and excessive black color (Andreão et al., 2020). A significant proportion of this agro-waste is being dumped in nearby regions more and more, which has a negative impact on the ecosystem and lacks disposal land (Bahurudeen et al., 2015). The main components of raw SA are coarse/fine fibrous unburned particles and fine burnt particles (Bahurudeen and Santhanam, 2015). This ash is irregularly shaped and primarily amorphous silica-rich after suitable processing to remove unburned components, with lesser amounts of aluminum, alkali, iron, and magnesium (Setayesh Gar et al., 2017). The analysis of the literature reveals that processed SA may be viewed as a supplementary cementitious material (SCM), and it is generally acknowledged that the fineness of SA enhances its pozzolanic properties (Le et al., 2018; Zareei et al., 2018).

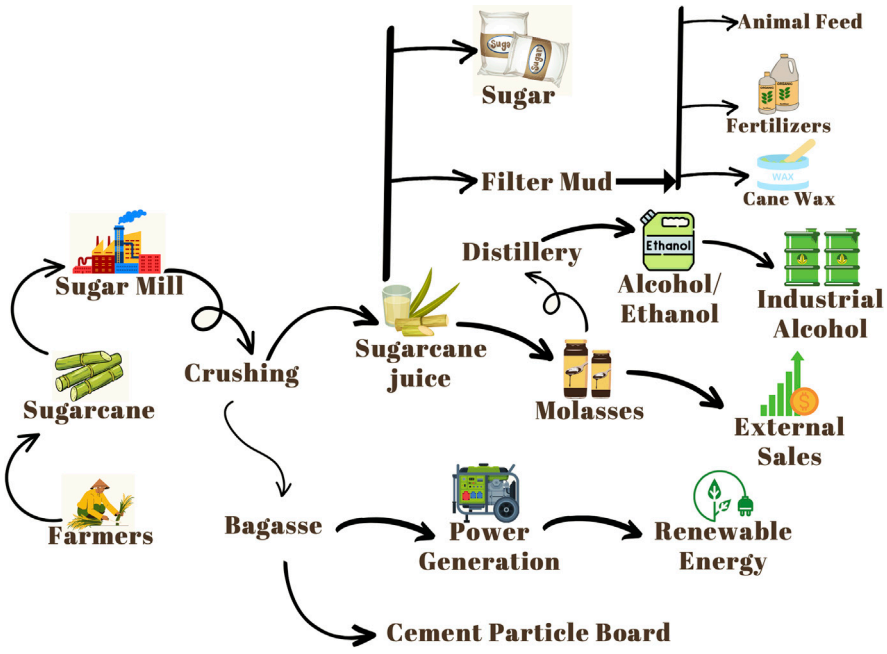


FIGURE 1
General schematic by-product of Sugar Cane.

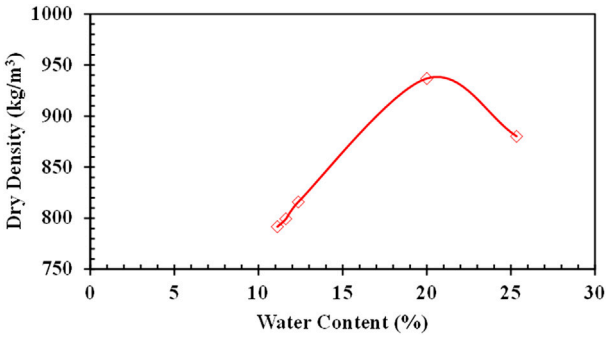


FIGURE 2
Compaction curve of sugarcane bagasse ash.

Alkali-activated materials (AAMs) have seen an increase in use as a Portland cement substitute in recent decades due to their advantages as a greener method. In-depth analyses of AAMs' effectiveness when it comes to mechanical strength, microstructure and durability have revealed results on par with or even better than those of ordinary Portland cement (OPC) (van Deventer et al., 2014). Alkaline activators and decent starting materials are used to create inorganic binders at the proper temperature. As activated solutions in the binder material, potassium/sodium hydroxides and/or sodium/potassium silicates are often favored (Duxson et al., 2006). Slag, fly ash, and coal bottom ash are examples of industrial by-products that include aluminosilicate and are widely utilized as precursors (Mugahed et al., 2022). Alkali hydroxide and/or alkali silicate solutions react chemically with solid aluminosilicate particles in the mixtures to generate binding gels. Two reaction products that differ from Portland cement in terms of their level of hydration are produced in AAMs, depending on the chemical components present in the starting materials. The reaction result may be N-A-S-H gels for low-calcium precursors such as fly ash (or similar ashes), and C-A-S-H gels for high-calcium precursors such as GBFS (Rakhimova and Rakhimov, 2014). Two important factors that significantly affect the compressive strength of a binder are the SiO2/Na2O molar ratio (also known as the silicate modulus, or Ms) and the Na2O molar concentration of the liquid. Based on the results of the experiments (Zhang et al., 2022a), the fresh mixtures can be classified as Bingham fluids, and the addition of the right amount of nano-SiO2 (NS) and water-reducing admixture can improve the mixtures' rheology and flowability. However, adding too much PVA fiber and NS has an negative effect on the mixtures' workability. According to reports, increasing the sodium oxide dose or the silicate modulus of the activator has led to better strength by improving raw material dissolution. Alkali-activated materials can be heat cured to increase their early strength and possibly reduce their shrinkage (Thomas et al., 2017). However, specimens with restricted fractures that were healed in water at room temperature showed a decrease of mechanical strength (Kirschner and Harmuth, 2004).

Furthermore, tiny particulates that might cause serious air pollution are present in the areas of sugar facilities. The majority of sugar factories are situated in villages, and SA (remaining sugarcane bagasse ash) from the factories is immediately deposited onto the arable land in these communities (Deepika et al., 2017). It is essential to discover another application for bagasse ash other than disposal. Bagasse ash has been suggested as a suitable ingredient for blended cement manufacture in earlier studies (Ganesan et al., 2007). Ashes with reactive silica are produced by the cogeneration boiler's carefully regulated combustion process (Cetin et al., 2004). According to research using differential scanning calorimetry (DSC), enhanced production of calcium-silicate-hydrate (C-S-H) gel occurred when SA is present (Singh et al., 2000). However, the use of unprocessed SBS as a cementitious material is hindered by the greater loss on ignition (LOI) value of around 20 percent and the lower specific gravity of about 1.9. Therefore, the majority of researchers agree that treating SA is preferred over increasing its pozzolanicity (Cordeiro et al., 2009).

In comparing SBS-blended concrete to regular Portland cement (OPC) concrete, it has demonstrated increased strength, decreased permeability, and low heat of hydration (Ganesan et al., 2007; Bahurudeen et al., 2015). Due to a lack of proper knowledge of the material and scalable methodologies, the manufacturing of building materials using bagasse ash has been prohibited (Mangi et al., 2020). Most past research studies have concentrated on using bagasse ash in concrete, and on the basis of thorough experimental plans, acceptable processing technology for blended cement manufacture has been recommended (Frías et al., 2011). Numerous studies have been conducted to determine the potential utility of SA in the major nations that produce sugar, including Brazil, India, and Thailand (Chusilp et al., 2009; Wen et al., 2022). The appropriate performance assessment and processing of bagasse ash for different building materials, such as alkali-activated concrete, paver blocks, and unburned bricks, were not sufficiently studied in previous research investigations. To gain a scientific understanding and make the most use of SA, performance evaluation in various applications is also required in addition to material characterization.

Sustainable concrete is popular as a building material because of its higher flexural and compressive strengths and lower cost. Due to its limited elasticity and resistance to fracture, it is naturally vulnerable. Metal or non-metal fibers have been put into concrete to address these issues. Fiber-reinforced concrete cracks cannot form or spread if the fibers are distributed randomly. Because of this, concrete is now far more robust and malleable (Wen et al., 2022). Structures prone to earthquakes, tunnel linings, and explosions have all made use of this material (Khawaja et al., 2021). Fibers are made of polyvinyl alcohol (PVA), polypropylene (PP), hooked-end steel fiber (HKs), crimped steel fiber (CRs), and others (Najm et al., 2022a). Metallic fibers (HKs and CRs) are the bestbecause of their strong compressive, tensile, twisting, and bridging strengths. PVA-reinforced concrete offers higher pull-out loads and flexural strength than concrete reinforced with metallic fibers. The inclusion of fiber also highly contributes to enhancing the fracture (Xu et al., 2018) and fire resistance (Yashwanth et al., 2017) and seismic load (Channa et al., 2022). According to the findings (Zhang et al., 2022b), the geopolymer mortar had considerable mass loss when exposed to temperatures between 25°C and 250°C, however, only a little amount of mass loss was observed between 250°C and 700°C and none at all between 700°C and 800°C. Under wet-thermal and chloride salt conditions, fiber-reinforced cementitious composites' fracture characteristics were enhanced by polyvinyl alcohol (PVA) and nano-SiO2 (NS). PVA fibre and NS enhanced the porosity, microcracks, and interfacial transition zone of fiber-reinforced cementitious composites at the microscopic level. The fracture characteristics considerably improved at 1.2% and 0.5%, respectively, of PVA fibre and NS contents (Zhang et al., 2022c) When the structure of PVA and fiber-reinforced

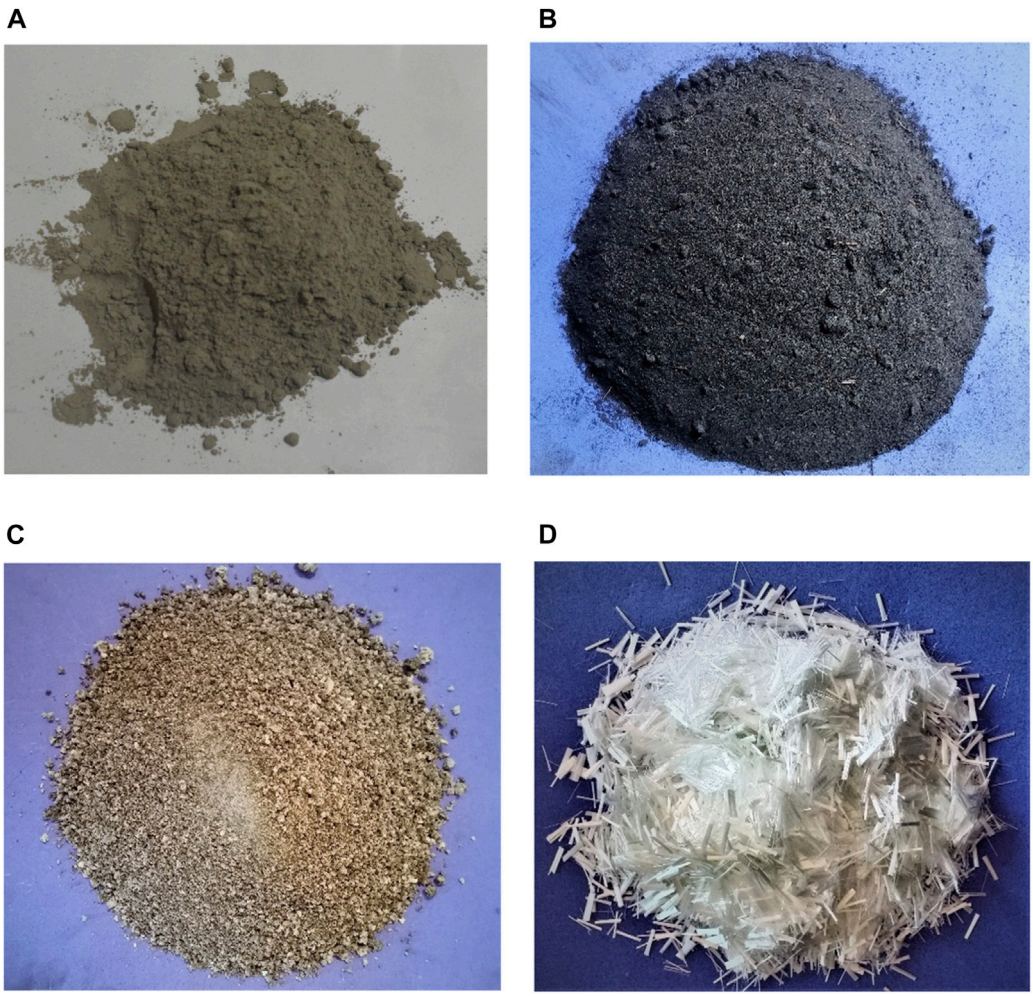


FIGURE 3
Materials used **(A)** OPC (53 Grade); **(B)** SA; **(C)** BFS; **(D)** GF.

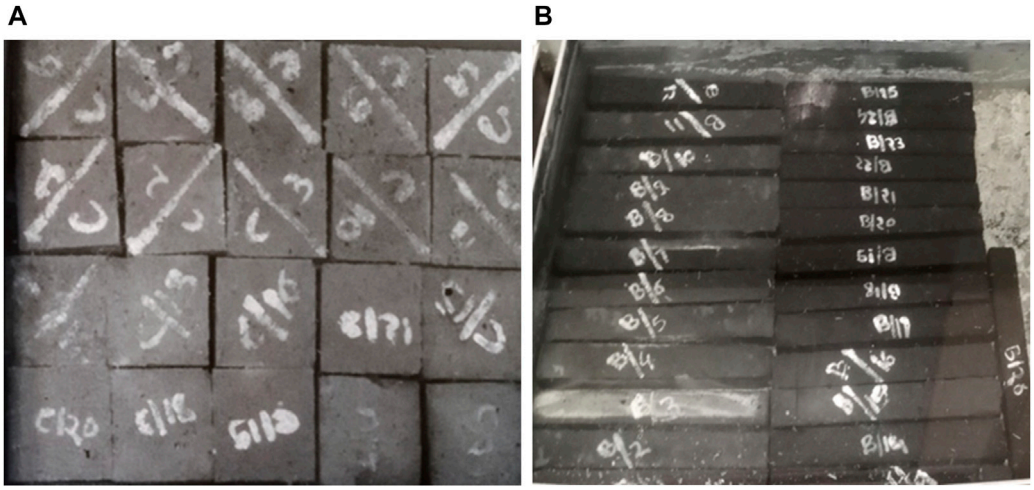


FIGURE 4
Curing of **(A)** cube specimen; **(B)** beam specimen.

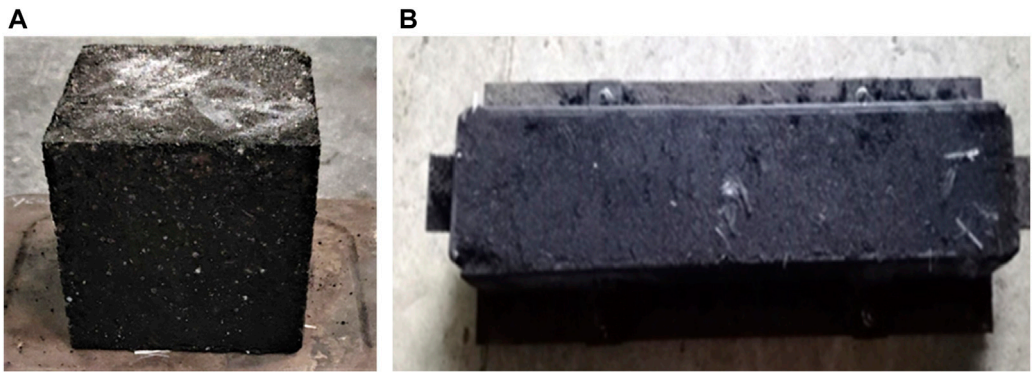


FIGURE 5
**(A)** Cube specimen (100 mm × 100 mm × 100 mm). **(B)** Beam specimen (400 mm × 50 mm × 50 mm).

**TABLE 1 Mix ratios and quantity of materials used for preparing cube and beam specimens.**

| No. | Mix ratio (%) | Weight of SA WSA (gm) | Weight of BF slag W BF slag (gm) | Weight of glass fiber W GF (gm) 10% cement | Weight of cement 10% Wc (gm) | Weight of cement 15% Wc (gm) | Weight of cement 20% Wc (gm) | Water, $V_w$ (mL) (55%) | Curing duration in days |
|---|---|---|---|---|---|---|---|---|---|
| 1 | 0.2 | 859.05 | 85.90 | 1.72 | 85.90 | 128.5 | 171.81 | 429.52 | 7, 14, 28 |
| 2 | 0.4 | 857.0 | 85.70 | 3.43 | 85.70 | 128.5 | 171.4 | 428.50 | 7, 14, 28 |
| 3 | 0.6 | 854.94 | 85.49 | 5.15 | 85.49 | 128.24 | 170.98 | 427.47 | 7, 14, 28 |
| 4 | 0.8 | 852.88 | 85.29 | 6.86 | 85.29 | 127.93 | 170.57 | 426.44 | 7, 14, 28 |
| 5 | 1.0 | 850.91 | 85.09 | 8.10 | 85.09 | 127.63 | 170.18 | 425.45 | 7, 14, 28 |
| 6 | 1.2 | 848.34 | 84.83 | 10.11 | 84.83 | 127.20 | 169.66 | 424.16 | 7, 14, 28 |

cementitious composite samples heated to 600°C and 800°C became loose and more microcracks formed, it was determined that the macro-mechanical properties had reduced (Zhang et al., 2022d).

According to the literature review, there have been various initiatives to use waste materials for sustainable development, such as coal ash, bottom ash, and stone dust in cement (Ram Rathan Lal and Badwaik, 2016; Ram Rathan Lal and Nawkhare, 2016). Very few works carried out with sugar cane bagasse ash in this direction. Consequently, the main goal of this work was to evaluate the effects of various quantities of geomaterial composites with glass fibres on the mechanical properties and classify them into geomaterials per the design standards for usability. Therefore, a detailed investigation into the compressive, flexural, density, tangent modulus, stress–strain pattern, and load–deflection curve of newly prepared materials was conducted. This in-depth analysis of sugar cane bagasse ash and blast furnace slag was done with the goal of finding the ideal ratio in terms of mechanical qualities and cost, reducing environmental stress, and pursuing sustainable growth. In the numerous studies in the literature, experimental works have been used to predict the behavior of sugar cane bagasse ash (Channa et al., 2022). However, there has been no experimental work to evaluate the effect of using sugar cane bagasse ash (SA) and blast furnace slag (BF) reinforced by glass fiber (GF) on the mechanical properties of mortar, which is crucial to calibrate under different loadings (compressive and flexural) and can be used as an indication for future studies based on sugar cane bagasse ash. In addition, several scholars used different variants of concrete in their numerical and experimental research works performed under quasi-static, static, and extreme loading conditions (Khan and El Rimawi, Forthcoming; Khan and Ali, 2016; Khan et al., 2017a; Khan et al., 2017b; Khan et al., 2017c; Khan et al., 2018; Khan and Ali, 2019; Ahmed et al., 2021; Anas et al., 2021; Anas et al., 2022a; Ahmed et al., 2022; Anas et al., 2022b; Khan et al., 2022; Mansouri et al., 2022; Qaidi et al., 2022; Anas et al., 2023; Iman et al., 2023).

## 2 Materials and methods

The performance of sugar cane bagasse ash reinforced with glass fiber (GF) in comparison to blast furnace slag (BF) and cement is examined in the current study. The compressive and flexural strength, density, tangent modulus, stress–strain pattern, and load–deflection curve of concrete are evaluated.

### 2.1 Materials

The research materials used consist of ordinary Portland Cement (OPC) 53 grade, sugar cane bagasse ash (SA), blast

**TABLE 2 Material testing mechanisms.**

| Tests | Equipment | Sample | Curing condition | Formula |
|---|---|---|---|---|
| Slump | Abram cone | Fresh concrete | Quickly after mixing | - |
| Compressive Strength (ASTM C39) | (2000 KN) Compressive testing machine at axial | Hardened concrete | 28 Days | $CS = \frac{P}{A}$ |
| Flexural Strength (ASTM C78) | Two-point load test | Hardened concrete | 28 Days | $FS = \frac{PL}{bd^2}$ |

*CS*, compressive strength, *A* = cross-sectional area, *FS*, flexural strength, *P* = maximum load from load deflection curve, *L* = span length, *b* = width of specimen, *d* = depth of specimen.

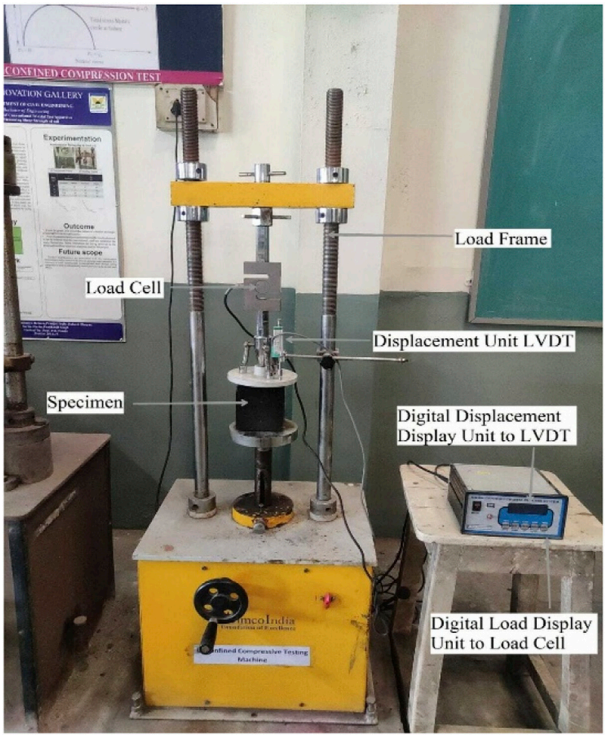


FIGURE 6
Compressive strength machine.

furnace slag (BFS), and glass fiber (GF). Bagasse ash was collected in a dry state from the Khambata Sugar Cane Factory, Bhandara (District), India. Blast furnace slag was collected in dry conditions from Varthi Steel Industries, Bhandara (District), India, and glass fiber was obtained from Jaipurkar Construction Pvt. Ltd., Nagpur (District), India.

The sugarcane bagasse ash used in this investigation had a chemical make-up of 45% cellulose, 27% hemicellulose, 20% lignin, and 8% ash, obtained from the Soil Science and Chemistry Department, Nagpur University, India. In the laboratory, the sugar cane bagasse ash's material characteristics were calculated. According to the Unified Soil Classification System (USCS), the sugar cane bagasse ash is categorized as analogous to fine sand and silt. Sugar cane bagasse ash may also be classified as non-plastic material that affects the granulometric behavior of clay particles (ASTM C1585-13, 2013). In accordance with the ASTM D 698 (ASTM D1557, 2021), the standard proctor experiment was used to determine the compaction characteristics of the material. The dry density of the sugar cane bagasse ash was 940 kg/m$^3$, and the moisture content was 20%. The compaction curve of the SA is plotted in Figure 2.

The blast furnace slag was determined to have a fineness modulus of 2.89, as per IS 383–1970 (BIS:383, 1970), and classified into a medium sand category. Glass fiber was used in the experiment for reinforcing the prepared material. Alkali-resistant (AR) glass fiber (dimensions: length of 12 mm and diameter of 19 μm) was used in the present work for an X-ray

**TABLE 3 Density of beam materials after 7, 14, and 28 days for 10%, 15%, and 20% cement to SA materials.**

| Mix ratio | 7 Days | | | 14 Days | | | 28 Days | | |
|---|---|---|---|---|---|---|---|---|---|
| | Cement % | | | Cement % | | | Cement % | | |
| | 10% | 15% | 20% | 10% | 15% | 20% | 10% | 15% | 20% |
| 0.2 | 1187.2 | 1225.4 | 1261.5 | 1237.2 | 1269.0 | 1291.0 | 1265.8 | 1292.1 | 1318.0 |
| 0.4 | 1172.1 | 1209 | 1241.9 | 1226.6 | 1255.0 | 1280.0 | 1257.1 | 1280.0 | 1305.0 |
| 0.6 | 1167.0 | 1198.3 | 1228.2 | 1217.8 | 1243.6 | 1268.9 | 1243.0 | 1268.2 | 1292.7 |
| 0.8 | 1153.1 | 1187 | 1217.9 | 1205.0 | 1231.8 | 1255.7 | 1231.3 | 1255.9 | 1280.0 |
| 1.0 | 1143.3 | 1173.9 | 1205.0 | 1192.3 | 1217.8 | 1242.0 | 1219.8 | 1243.0 | 1268.9 |
| 1.2 | 1136.9 | 1165.7 | 1197.4 | 1185 | 1205.0 | 1231.1 | 1207 | 1231.7 | 1259.6 |

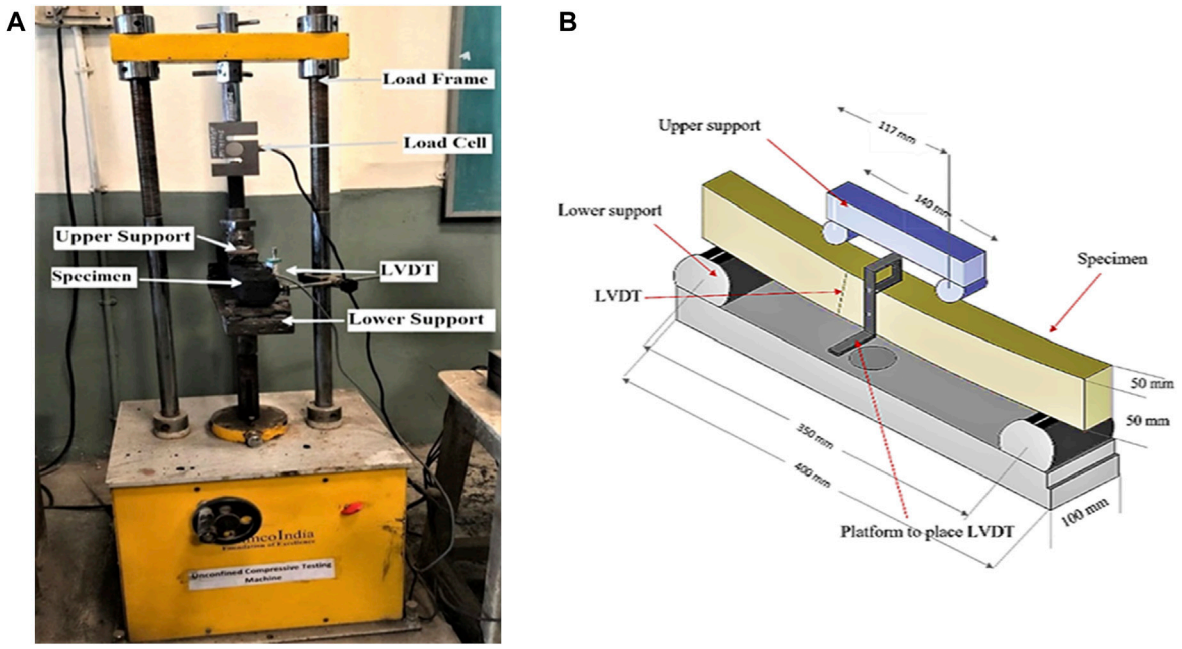


FIGURE 7
Dimensions of the fabricated tool for flexural test. **(A)** Real Dimensions; **(B)**Sketch Dimension.

fluorescence (XRF) trial and was executed using an X-ray fluorescence spectrometer at the Indian Bureau of Mines, Nagpur. As per ASTM C618 (ASTM C618-17a, 2017), sugar cane bagasse ash is classified as a Class F type of material, and blast furnace slag is classified as a Class C type of material. Figure 3 shows the materials used in the research work: OPC (53 grade), sugar cane bagasse ash, blast furnace slag, and glass fiber.

## 2.2 Preparation of specimen

The quantities of various constituents of the mix were calculated based on a method used by previous researchers (Nikhade and Lal, 2021). The weight ratio of glass fibre to sugarcane bagasse ash is known as the mix ratio %. In the current study, the dry weight of SA is calculated using formula WSA = $\gamma_{dmax}$ x VSA, where $\gamma_{dmax}$ maximum dry unit weight of sugar cane bagasse ash and VSA is volume of SA, VSA = V-VBF–VGF, V the total volume to specimen (1000 $cm^3$), and VBF is taken 70 $cm^3$ and volume of VGF glass fiber is taken 2.3 $cm^3$ to achieve the mix ratio 0.2%.The ratios were 0.2, 0.4, 0.6, 0.8, and 1.0% for the cube specimens and 0.2, 0.4, 0.6, 0.8, 1.0, and 1.2% for the beam specimens. To achieve a mix ratio of 0.2, the volume of the blast furnace was 70 $cm^3$ and that of the glass fiber was 2.3 cc. After mixing the materials, i.e., the SA, BF slag, GF, and cement, the materials were formed into a homogeneous slurry with an optimum moisture content of 20%, and the water to sugar cane bagasse ash ratio was maintained at 55% for the present work.

## 2.3 Curing method adopted

Curing is a process used to control the hydration that occurs in concrete due to the presence of Portland cement. The majority of the time, it entails controlling the loss of moisture and, in some instances, temperature (ASTM Standards C-293, 2002). Examples of curing techniques include using shade during concrete work, covering concrete surfaces with hessian or gunny bags, water spraying, the ponding process, immersion in water, membrane curing, and steam curing (Maroliya, 2012). Immersion curing was chosen for this project (Figure 4) at room temperature (25°C–30°C), where the samples were submerged entirely in water. This is a suitable approach that satisfies all curing requirements, including hydration promotion, shrinkage elimination, and heat absorption during hydration.

## 2.4 Mix proportions

In the container, the required amounts of SA, BF slag, and cement were obtained and mixed thoroughly with the required amount of water. After that, glass fiber was added to the mix to prevent it from clustering. The casting of the specimens was performed immediately after the mixing was completed. A total of 135 cube specimens (100 mm × 100 mm × 100 mm) and 162 beam specimens (400 mm × 50 mm × 50 mm) were prepared. After 24 h, the specimens were taken out from the molds, and air dried again for a period of 24 h, as shown in Figure 5A, B. The mix ratios and material amounts needed to make the cube and beam specimens are shown in Table 1.

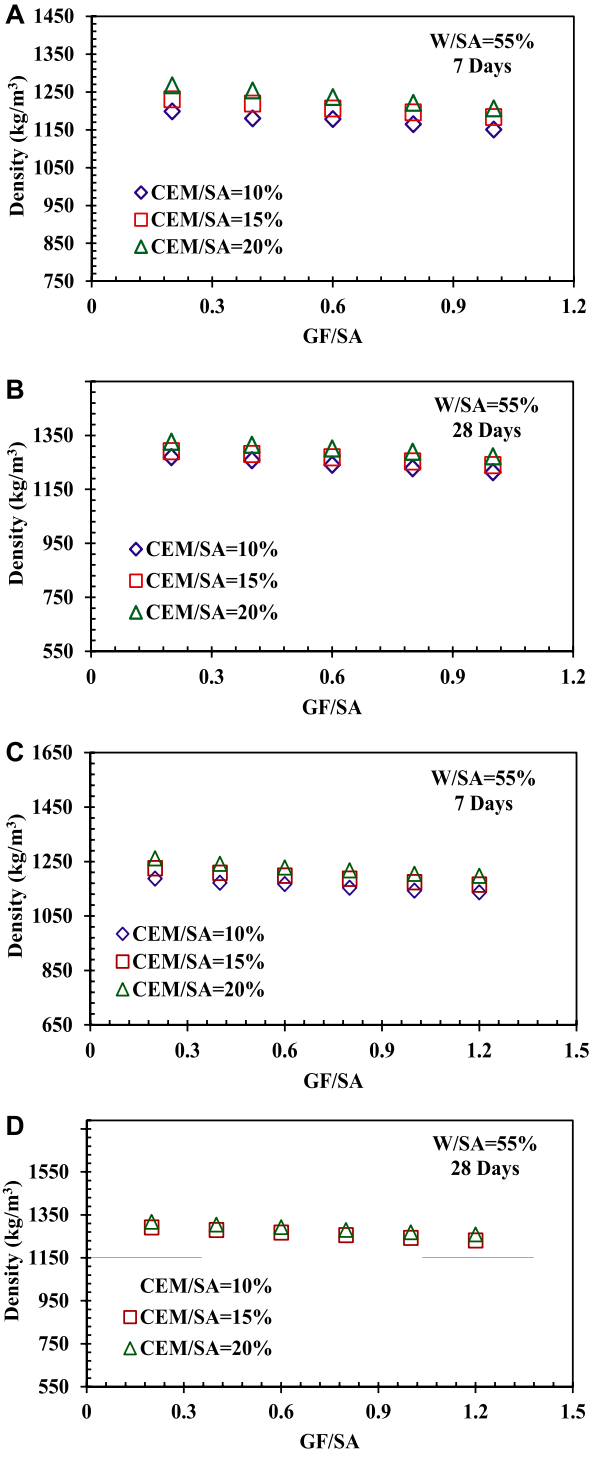


FIGURE 8
Density of prepared materials for **(A)** 7 days and **(B)** 28 for cubes; **(C)** 7 days and **(D)** 28 days for beams with respect to the mix value.

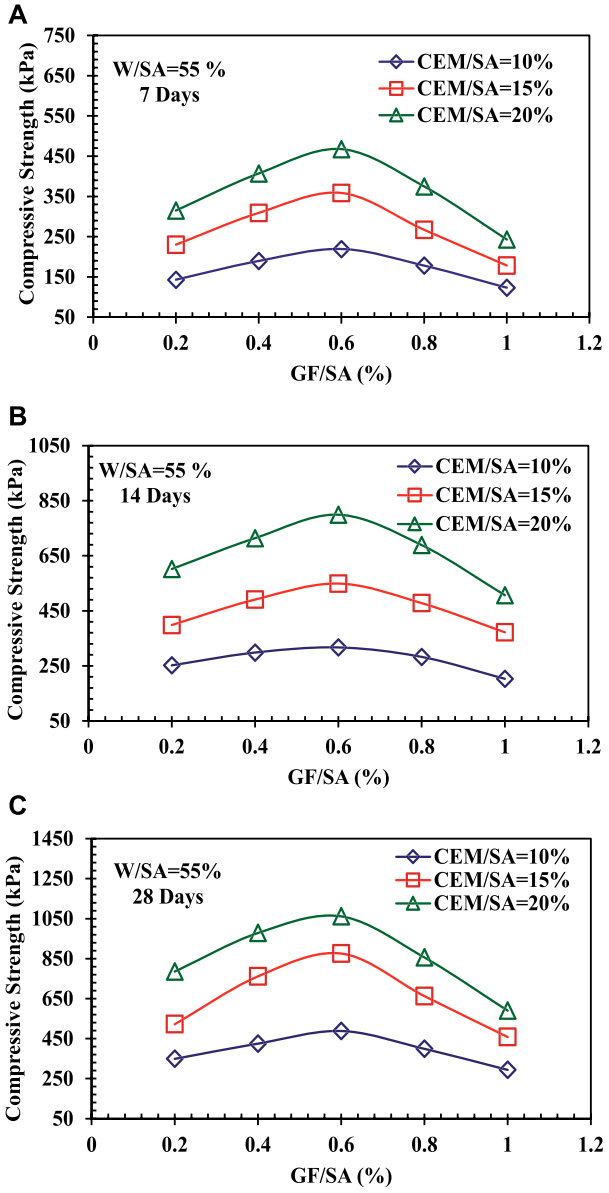


FIGURE 9
Compressive strength of prepared materials for **(A)** 7 days; **(B)** 14 days; and **(C)** 28 days with respect to mix value.

## 2.5 Tests on mechanical properties

### 2.5.1 Compressive strength test

The compressive strength of a geomaterial is defined as its ability to withstand failure when subjected to compressive pressures. The load applied at the point of failure is divided by the cross-sectional area of the sample to determine the hardened concrete's compressive strength (Table 2). The samples were tested using a compressive strength testing device in accordance with ASTM C39 after 28 days of curing (ASTM C39, 2016) (Figure 6).

### 2.5.2 Flexural strength test

As per ASTM C78, this flexural strength test was performed (ASTM C78, 2016). Figure 7A, B shows the experimental setup of a 2-point bending problem fabricated for flexural testing; the base support was 100 mm wide and 400 mm long, and it was attached to a metal block. Three hundred 50 mm was the effective length between the metal blocks arranged in a grid.

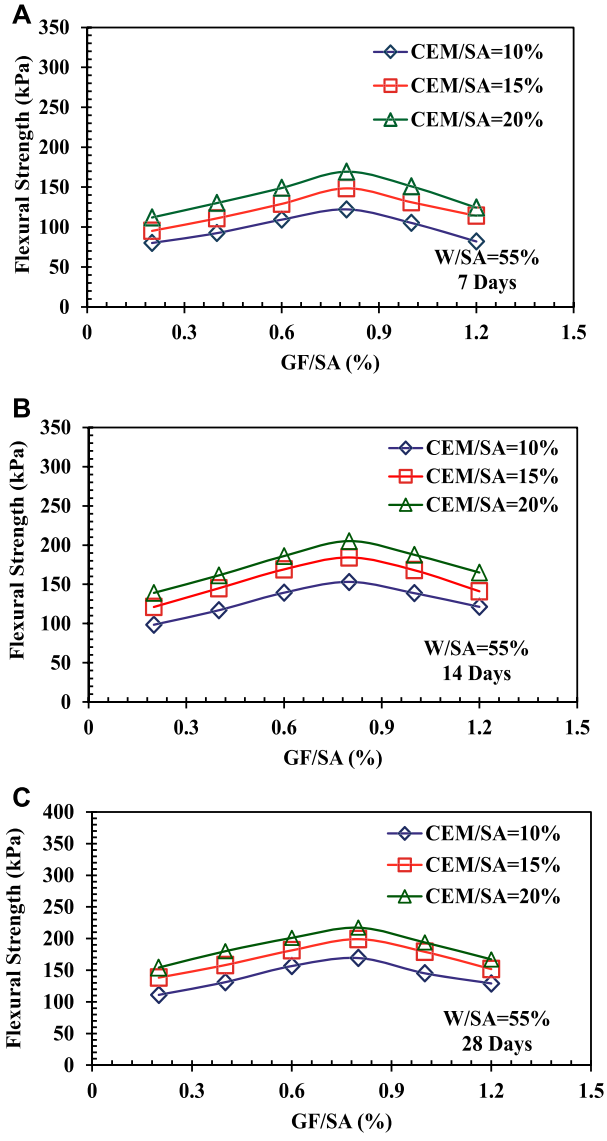


FIGURE 10
Flexural strength of prepared materials for **(A)** 7 days; **(B)** 14 days; and **(C)** 28 days with respect to mix value.

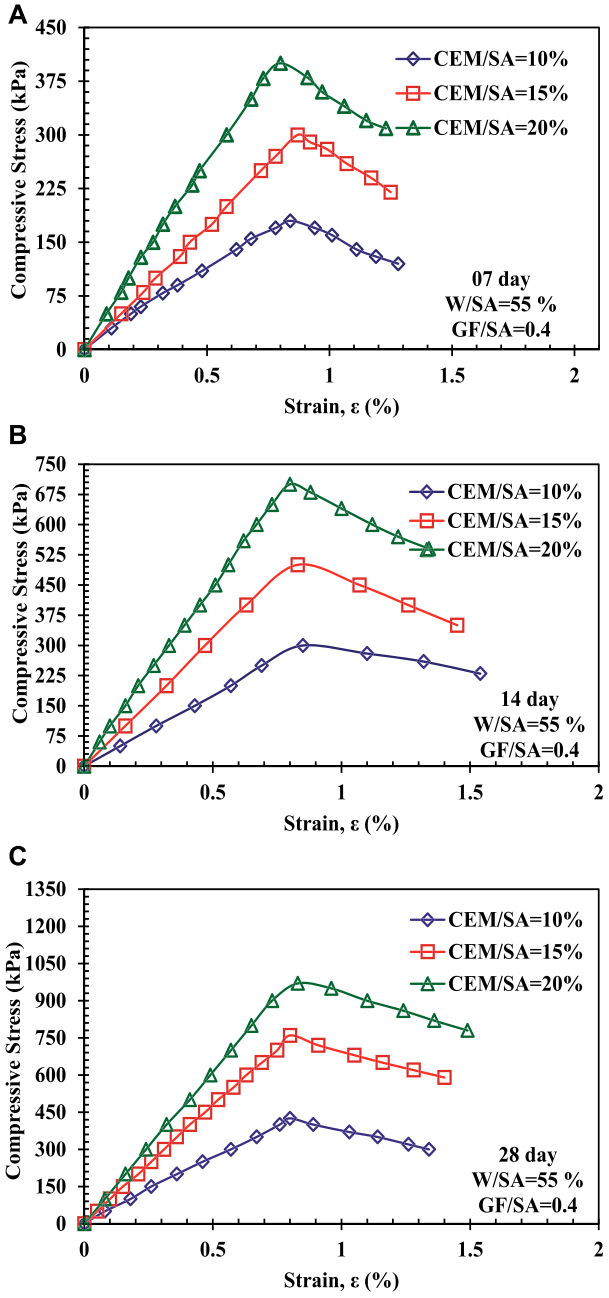


FIGURE 11
Stress–strain curve of SA and BF slag reinforced with glass fiber under compressive stress for mix ratios of 0.4% for **(A)** 7, **(B)** 14, and **(C)** 28 days.

## 2.6 Tests on microstructural analysis

### 2.6.1 Scanning electron microscopy

Scanning electron microscopy (SEM) uses image analysis to measure and evaluate minute details by repeatedly scanning the surface of a material with a concentrated electron beam. The signals generated when electrons collide with atoms in a sample reveal clues about the surface's topography and composition. Using an SEM, one can look into component failures, find particles, and examine substance–substrate interactions (ASTM C78, 2016). A JEOL JSM6380 LV scanning electron microscope with an accelerating voltage of 30.0 kV was used for this work. The materials were gold-plated in order to conduct energy dispersive spectroscopy (EDS).

### 2.6.2 X-ray diffraction

In order to learn about and identify the atomic and crystallographic nature of a material, X-ray diffraction (XRD) is performed as a microstructural analysis test. Exiting X-rays are irradiated onto a sample, and their intensities and scattering angles are measured. The material's composition is ascertained by examining the position, angle, and intensities of the scattered intensity peaks, which are presented as a function of the scattering angle. In geological research, XRD is frequently

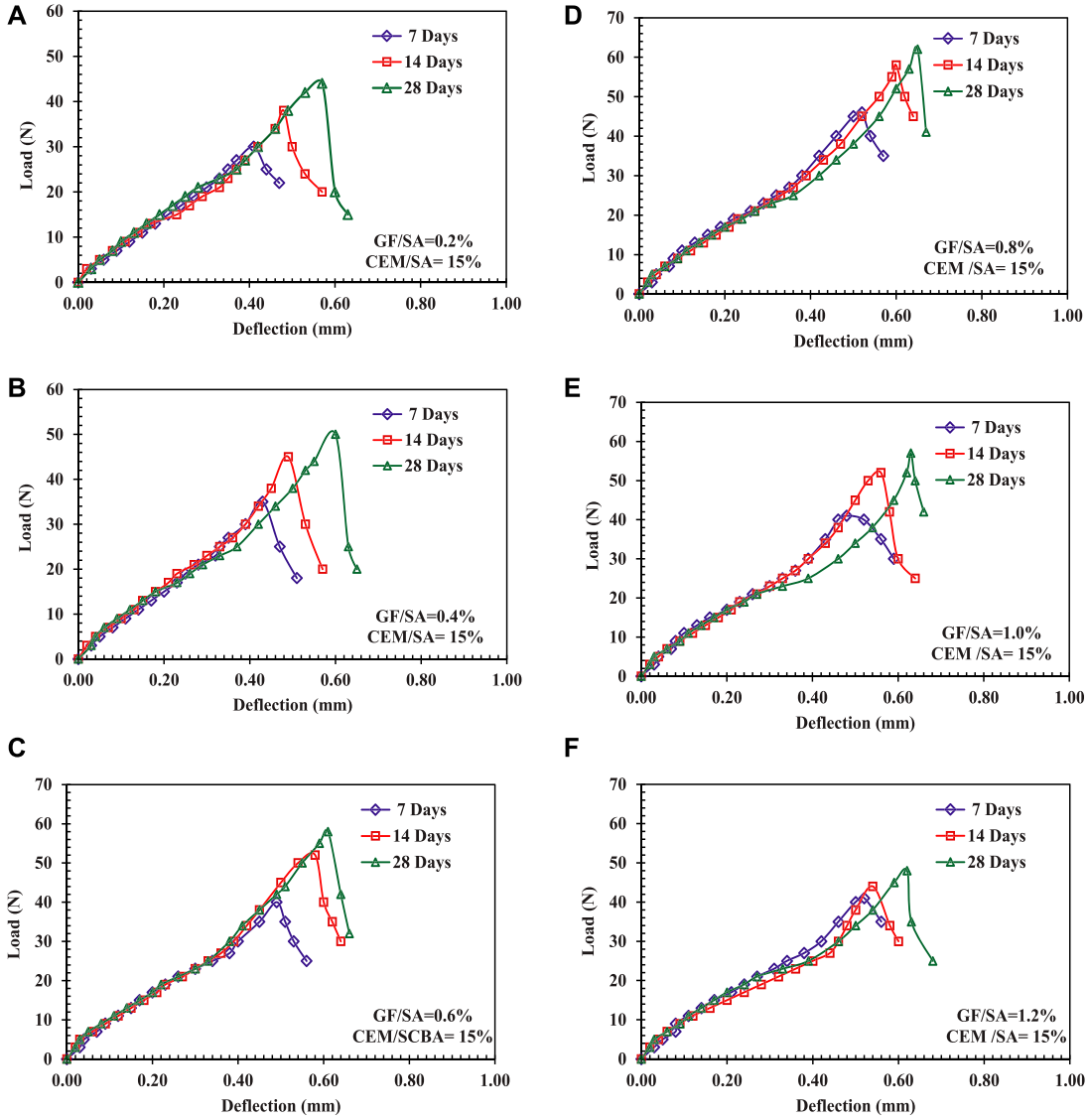


FIGURE 12
Load vs. deflection curve of prepared materials for all curing periods at GF/SA mix ratios of **(A)** 0.2%; **(B)** 0.4%; **(C)** 0.6%; **(D)** 0.8%; **(E)** 1.0%; **(F)** 1.2%, and CEM/SA ratio of 15%.

combined with other microstructural techniques, such as electron microprobe microscopy, scanning electron microscopy and optical light microscopy particularly when the sample to be investigated is a combination. XRD data can be used to identify each mineral present in the sample and their relative abundance (Maroliya, 2012).

# 3 Result and discussion

The failure pattern, stress and strain pattern, density, initial tangent modulus, compressive strength, flexural strength, and load–deflection curve pattern of the cube and beam specimens were evaluated, and the results obtained are discussed.

## 3.1 Density of specimen

The cube and beam specimens were weighed after air drying, and the densities were calculated before the compressive strength tests. It was observed that for all mix ratio percentages, the density of the materials decreased with increases in the mix ratio percentages for all curing periods, as shown in Figure 8. For each mixing ratio, the density of the compression cube specimens increased with the percentage of the cement to sugar cane bagasse ash ratio increasing from 0% to 20%. The density of the material used for the cube specimens varied from 1140.0 kg/m$^3$ to 1320.1 kg/m$^3$ and for the beams, it varied from 1136.9 to 1318 kg/m$^3$. The density of the materials was higher at a 0.2% mix ratio and lower at a 1.2% mix ratio. At a

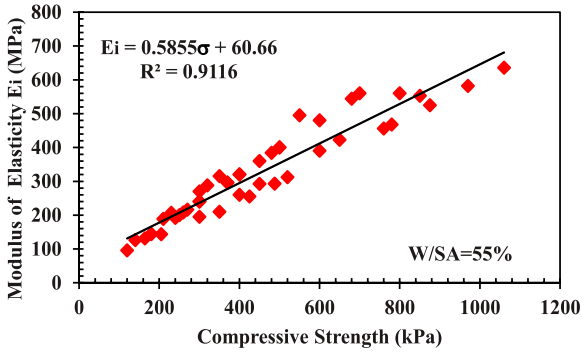


FIGURE 13
Association between initial tangent modulus and compressive strength.

10% cement-to-bagasse ash mix ratio, the density of the material used to prepare the cube specimens ranged from 1195.7 kg/m$^3$ to 1140.0 kg/m$^3$ and the percentage change at 7 days of curing was 4.65%. For the beam material, the density varied from 1187.2 kg/m$^3$ to 1136.2 kg/m$^3$, and the percentage change in density at 7 days of curing was 4.29%. Table 3 summarizes the density of the beam materials after 7, 14, and 28 days for 10%, 15%, and 20% ratios of cement-to-SA materials. The density of the materials obtained in the present study lies within the range of lightweight filler materials, i.e., between 700 kg/m$^3$ and 1100 kg/m$^3$, as indicated by Nikhade et al. (Nikhade and Lal, 2021). The density of the materials was higher than in the study by Horvath (Osei et al., 2020), of which it was in the range of 12–32 kg/m$^3$.

## 3.2 Compressive strength

The compressive strengths of the GF-reinforced SA and BF slag-based specimens were remarkably influenced by the curing time, mix rate, and ratios of the cement to SA. The peak magnitude achieved in the compressive stress curve was taken as the compressive strength. It was found that the addition of GF to SA improved the compressive strength until an optimum percentage of fiber mix. For each of the mix ratios and curing periods, the specimens with a 0.6% mix ratio had the maximum compressive strength. Similar behavior was observed for the blast furnace slag material prepared by Nikhade et al. (Mandal et al., 2018; Nikhade and Lal, 2023). The value of compressive strength ranged from 120 kPa to 1055.5 kPa. The compressive strength of the material after 7 days of curing was 140.0 kPa at a mix ratio of 0.2% and increased up to 219.3 kPa with a mix ratio of 0.6%. Further increases in the mix ratio caused the compressive strength to decrease. The percentage increase in the compressive strength after 7 days of curing was 36.16%. Figure 9 demonstrates the variation in the compressive strength of the materials after 7 days, 14 days, and 28 days with respect to the mix value. A non-linear pattern was observed between the compressive strength and the mix ratio percentage for the curing period of 7–28 days. The strength values obtained in the study are higher than those in the study by Nikhade et al. (Nikhade and Lal, 2021), i.e., 100–500 kPa, which fall under the category of lightweight filler materials and between those in the study by Mandal D. (Mandal et al., 2018), i.e., 159 kPa–2500 kPa.

## 3.3 Flexural strength

The flexural strength of the prepared materials was also significantly influenced by the curing period, mix ratio, and

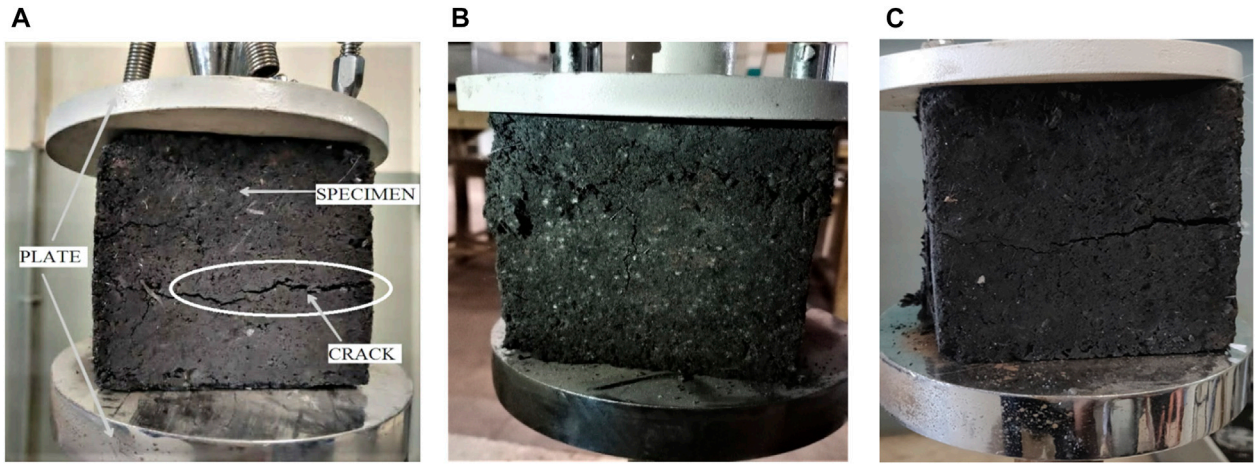


FIGURE 14
Development of cracks in cube specimens **(A,B, and C)**.

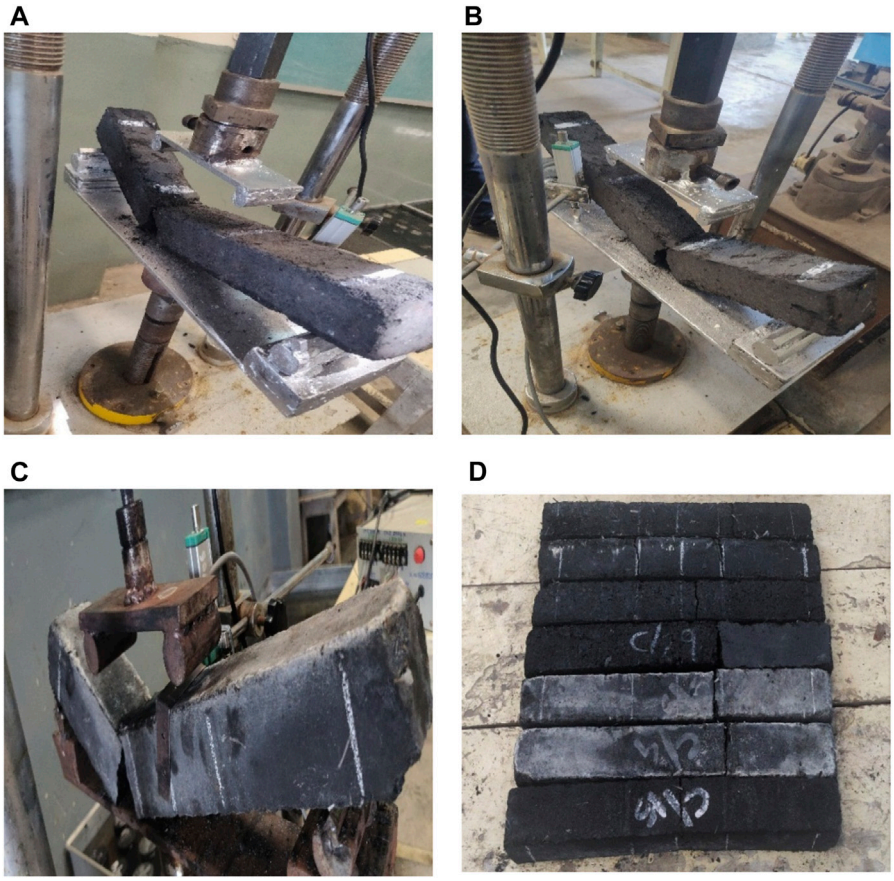


FIGURE 15
Development of cracks in beam specimens **(A–D)**.

percentage of GF used for the preparation of beam specimens for flexural tests. The flexural strength was obtained at the maximum failure load from the load–deflection curve. In all the specimens, the fracture occurred within the middle third of the span. The flexural strength was calculated according to ASTM C1609. The lowest value of flexural strength was 80.1 kPa, obtained at 7 days for the 0.2% mix ratio. The highest value of flexural strength was 217.2 kPa, obtained at 28 days for the mix ratio of 0.8%. Figure 10 shows the variation in the flexural strength with respect to the mix ratio. A non-linear relationship was found between the mix ratio and the flexural strength for all mix ratios and curing periods. However, the flexural strength increased with an increase in the percentage of glass fiber up to a certain extent. The highest or optimum value of the mix ratio was found to be 0.8%, at which the flexural strength was the maximum in all cases (Najm et al., 2022b; Najm and Ahmad, 2022; Nanayakkara et al., 2022).

## 3.4 Stress–strain curve

The significance of the stress–strain diagram is that the elastic modulus is calculated at a point on the ascending branch of the diagram. Figure 11 shows the stress–strain diagram for a mix ratio of 0.2% for 7, 14, and 28 days at the water-to-SA ratio of 55% plotted under a sustained strain rate of 1.00 mm/min in proportion to the BF slag reinforced with glass fiber at different mix ratios. For all specimens, a non-linear connection between stress and strain was found. It was observed that the CEM/SA at 20% had a higher stiffness compared to that at 10% and 15%. The material behavior of the geomaterial changed from ductile to brittle in nature for all the curing periods and mix ratios tested.

## 3.5 Load and deflection curve

The load–deflection curve was plotted for the cement-to-SA ratios of 10%, 15%, and 20%. The graph grows linearly up to the cracking load and then falls rapidly. The maximum load was found to increase with the curing periods for all specimens. The mid-span deflection at failure varied from 0.12 to 0.84 mm. Figure 12 shows the load–deflection relationships for GF/SA with 0.2%–1.2% mix ratios and the cement-to-SA ratio fixed at 15%. It was observed that the stiffness increased with the curing period and mix ratio, and higher stiffness at a 0.8% mix ratio was observed. The stiffness of the geomaterial for the cement-to-SA ratio of 20% was significantly higher than the other two combinations of cement percentages, i.e., 10% and 15%.

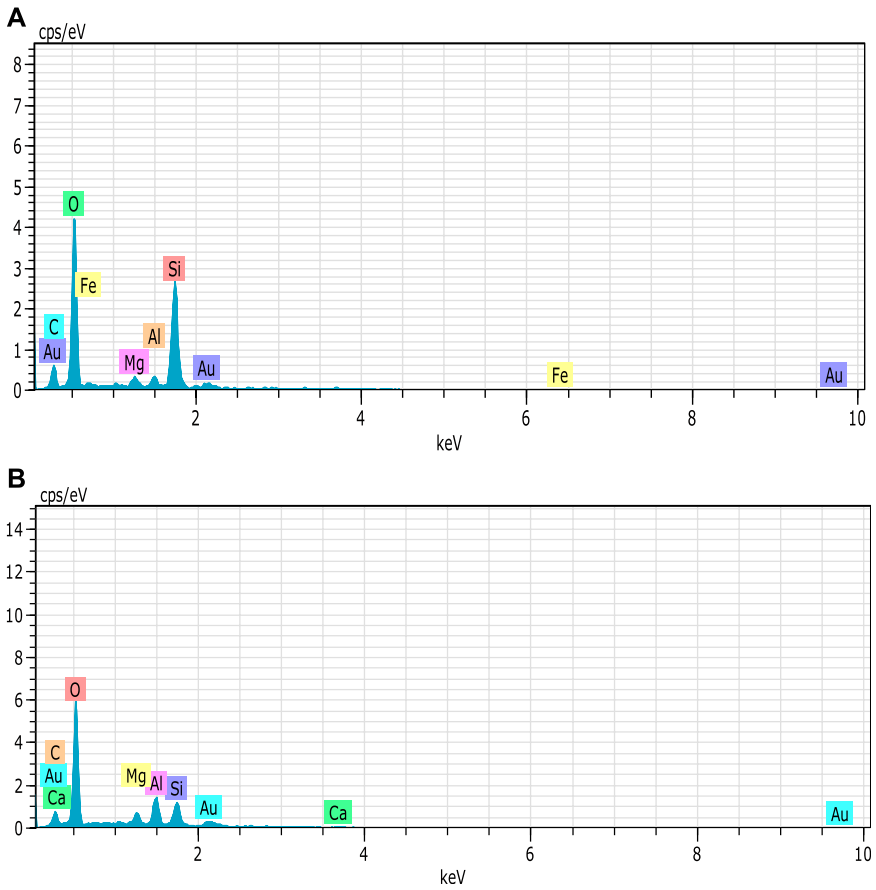


FIGURE 16
EDS patterns of **(A)** sugar cane bagasse ash; **(B)** blast furnace slag.

## 3.6 Initial tangent modulus

The initial tangent modulus ($E_i$) is a significant parameter that represents the rigidity of the prepared material. It was calculated as the incline of the tangent line to the rise of the stress–strain pattern. The ($E_i$), magnitude ranged from 96 to 636 MPa. The values obtained lie in the range of the lightweight filler category of materials, i.e., 79–555 MPa, as prepared by Liu et al. (Liu et al., 2006). The values are greater than those of the geofoam blocks prepared by Horvath (Horvath, 1998), i.e., in the range of 2.2–11.4 MPa. Figure 13 shows the association between the initial tangent modulus and the compressive strength. The connection between the ($E_i$) and the compressive strength ($\sigma$) is effectively represented by a linear relationship as follows.

## 3.7 Failure pattern

The failure patterns indicate that the cube specimens went through lateral expansion (bulging) before developing cracks in distinct planes, as shown in Figure 14A–C and Figure 15A–D. In the present experimental study, for most of the cube specimens, horizontal cracks occurred at locations around the bottom third of the specimen. Specimens tested for compression failed within an axial strain range of 0.6%–1.21%. For the beam specimen under flexural loading, vertical flexural crack developed at the pure flexural region (the span between two-point loads). All the specimens failed at deflection ranging from 0.16 to.

## 3.8 Microstructural analysis

The energy dispersive spectroscopy (EDS) test was performed on SA and BF slag materials to determine the phase composition materials. The minerals present in the sugar cane bagasse ash were identified using the database of JCPDS. The predominant minerals present in the SA and BF slag were quartz (81.13%), potassium carbonate (11.18%), cristobalite (4.0%), gumbelite (56.12%), and dolomite (32.12%). The EDS patterns of the SA and BF slag show the presence of oxygen, silica, and copper, as shown in Figure 16A, B. The SA materials consisted of irregularly shaped particles, the BF slag consisted of rounded, semi-spherical, and irregularly shaped particles and the glass fiber consisted of rounded-shape particles, as shown in Figure 17A–C. Finally, more or less similar mechanical and microstructural behaviors of waste material replacements reinforced by different types of fibers have been reported by several researchers (Horvath, 1998; Liu et al., 2006; Matsuda et al., 2008; Landa-Ruiz et al., 2021; Althoey et al., 2022; Najm et al., 2022b; Memon et al., 2022; Nanayakkara et al., 2022; Prabhath et al., 2022).

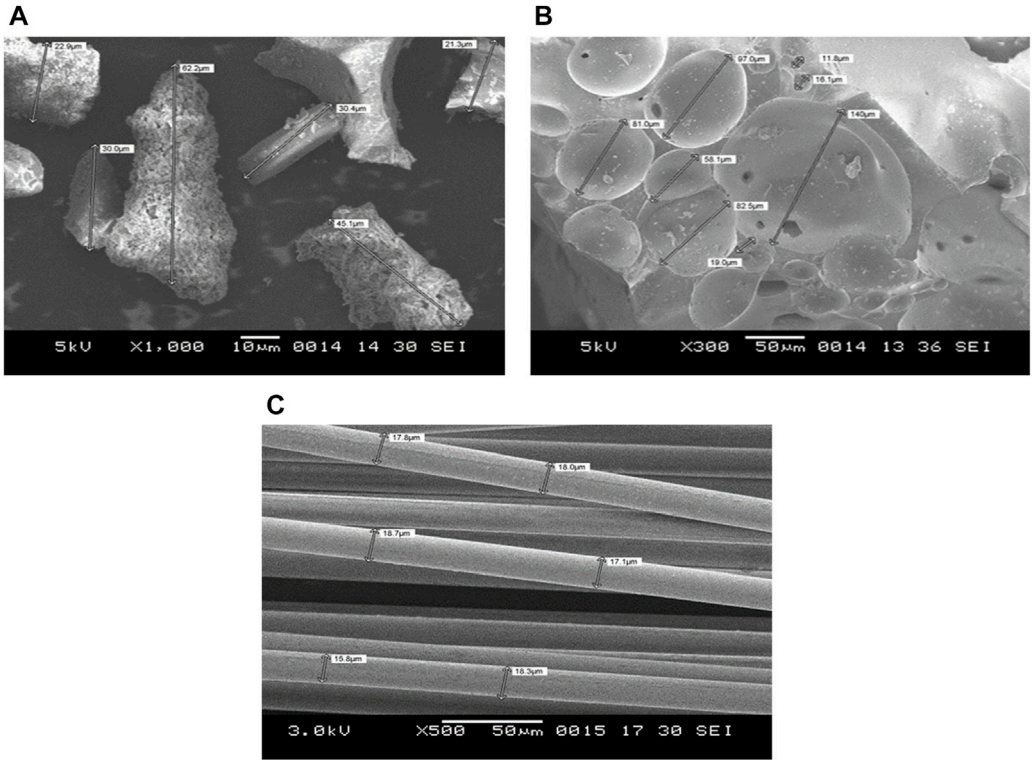


FIGURE 17
Microstructures of **(A)** SBCA; **(B)** BFS; **(C)** GF.

## 4 Limitation and future scope

Since a lower percentage of C/SA results in a specimen that does not retain its shape even after the curing period, and this value was used as 10% while making specimens for the compressive and flexural tests. Because of this restriction, no samples with cement contents less than 10% could be cast and analyzed. Further utilization of larger specimens is impossible because of the loading frame and testing instrument with the maximum size. Based on future research, the shear strength of a material can be determined under various compression and flexure loading conditions.

Additionally, the inclusion of nano-material admixtures (Khan et al., 2021) may further me used to enhance the properties and how the application of external strengthening (Khan, 2021a; Khan, 2021b; Khan, 2022) will affect failure modes may also be studied.

## 5 Conclusion

Sustainable concrete is popular as a building material because of its higher flexural and compressive strengths and lower cost. Due to its limited elasticity and resistance to fracture, it is naturally vulnerable. Metal and non-metal fibers have been put into concrete to address these issues. However, This study's primary goal was to evaluate the performance of various quantities of glass-fiber-reinforced geomaterial composites on the mechanical properties and classify them into geomaterials per the design standards for usability. Therefore, a detailed investigation into the compressive strength, flexural strength, density, tangent modulus, stress–strain pattern, and load–deflection curve of newly prepared materials were analyzed. The intention of such a detailed examination of sugar cane bagasse ash and blast furnace slag was to obtain the optimum contents in terms of mechanical properties to reduce environmental stress, and to approach sustainable development. So, in order to comprehend the behaviour of geomaterials created utilizing bagasse ash, an experimental investigation was carried out. From the observations, the findings are as follows.

– The density of the cube specimens decreased with increases in the mix ratios with values ranging from 0.2% to 1.0%. For the compression specimens with 20% cement and a water-to-SA ratio of 55%, the density decreased from 1320.1 to 1265 kg/m$^3$ (about 4.35%).
– The density of the beam specimens decreased with increases in the mix ratio values from 0.2% to 1.2%. For the flexural specimens with 20% cement content, the density decreased from 1318 to 1259.6 kg/m$^3$. The percentage decrease was about 4.43%.
– As the curing time went on, the compressive strength increased. The maximum compressive strength of 1055.5 kPa was found at 28 days for a mix ratio of 0.6% with a 20% CEM/SA ratio and a 55% W/SA ratio. The lowest compressive strength of 120 kPa was found at 7 days for a mix ratio of 1.0% and a CEM/SA ratio of 10%.
– Additionally, it was discovered that the flexural strength increased as the curing time increased. The highest flexural strength of

217.2 kPa was observed for the specimen with a mix ratio of 0.8% cured for 28 days, and a CEM/SA ratio kept at 20%. The lowest flexural strength of 80.10 kPa was observed for specimens with a mix ratio of 0.2% cured for 7 days with a CEM/SA ratio of 10%.

– The uniaxial compressive stress–strain curve shows non-linear behavior and increases in the compressive strength and stiffness were observed with an increase in the curing period. The failure strain ranged from 0.6% to 1.21% for a W/SA ratio of 55%.

– A non-linear relationship between the flexural load and the mid-span deflection was also observed. The curve increased linearly up to the failure load and then fell rapidly. The mid-span deflection at failure varied from 0.16 to 0.79 mm.

– The initial tangent modulus was found to vary linearly with compressive stress. The compressive stress varied non-linearly with the mix ratio; therefore, the initial tangent modulus varied non-linearly with the mix ratio. The value of the initial tangent modulus for the cube specimens ranged from 96 to 636 MPa for a W/SA ratio of 55%.

The obtained compressive strength in this research is more than 50 kPa as reported by Matsuda et al. (2008) (Matsuda et al., 2008), would resist liquefaction during an earthquake. Therefore, the newly developed SA reinforced glass fiber material satisfy the criteria and it can be used as fill materials which can solve the problem of environmental pollution with an eye on sustainable development. The materials prepared in this study are under the lightweight category of materials. Therefore, given the observations and the recommendations of the design standards, the geomaterial composite prepared in this study is suitable as a lightweight geomaterial.

## Data availability statement

The raw data supporting the conclusion of this article will be made available by the authors, without undue reservation.

## Author contributions

Conceptualization, HN and RL; data curation, HN, RL, KA, HMN, MM, MK, SA, MAH, and SI; formal analysis, HN, RL, KA, HMN, MM, MK, SA, MAH, and SI; funding acquisition, MAH, SA, MM, and SI; investigation, HN and RL; methodology, HN, RL, KA, and HMN; resources, KA, HMN, MM, MK, SA, MAH, and SI; software, HN, KA, and MK; supervision, RL; validation, RL, HMN, SA, MAH, and SI; visualization, HMN, SA, MAH, and SI; writing–original draft, HN and KA; writing–review and editing, MK, RL, HN, and HMN. All authors have read and agreed to the published version of the manuscript.

## Funding

The authors extend their appreciation to the Deanship of Scientific Research at King Khalid University, Abha, Kingdom of Saudi Arabia for funding this work through Large Groups RGP.2/209/44.

## Acknowledgments

The authors extend their appreciation to the Deanship of Scientific Research at King Khalid University, Abha, Kingdom of Saudi Arabia for funding this work through Large Groups RGP.2/209/44.The authors would like to thank the academic institutions YCCE, Nagpur, and KITS Ramtek for providing help.

## Conflict of interest

The authors declare that the research was conducted in the absence of any commercial or financial relationships that could be construed as a potential conflict of interest.

## Publisher's note



## References

Ahmed, H. U., Mohammed, A. A., Serwan, R., Mohammed, A. S., Mosavi, A., Sor, N. A. H., et al. (2021). Compressive strength of sustainable geopolymer concrete composites: A state-of-the-art review. *Sustainability* 13 (24), 13502. doi:10.3390/su132413502

Ahmed, H. U., Mohammed, A. S., Faraj Rabar, H., Qaidi, S. M. A., and Mohammed, A. A. (2022). Compressive strength of geopolymer concrete modified with nano-silica: Experimental and modeling investigations. *Case Stud. Constr. Mater.* 16, e01036. doi:10.1016/j.cscm.2022.e01036

Althoey, F., Awoyera, P. O., Inyama, K., Khan, M. A., Mursaleen, M., Hadidi, H. M., et al. (2022). Strength and microscale properties of bamboo fiber-reinforced concrete modified with natural rubber latex. *Front. Mater* 9, 1064885. doi:10.3389/fmats.2022.1064885

Anas, S. M., Alam, M., and Shariq, M. (2023). Damage response of conventionally reinforced two-way spanning concrete slab under eccentric impacting drop weight loading. *Def. Technol.* 19, 12–34. doi:10.1016/j.dt.2022.04.011

Anas, S. M., Alam, M., and Umair, M. (2021). Experimental and numerical investigations on performance of reinforced concrete slabs under explosive-induced air-blast loading: A state-of-the-art review. *Structures* 31, 428–461. doi:10.1016/j.istruc.2021.01.102

Anas, S. M., Alam, M. I., Haytham, F., Najm, H. M., and Sabri, M. M. S. (2022). Role of cross-diagonal reinforcements in lieu of seismic confining stirrups in the performance enhancement of square RC columns carrying axial load subjected to close-range explosive loading. *Front. Mater.* 9. Article in press. doi:10.3389/fmats.2022.1002195

Anas, S. M., Alam, M. I., Haytham, F., Najm, H. M., and Sabri, M. M. S. (2022). Ultra high performance concrete (UHPC) and C-frp tension Re-bars: A unique combinations of materials for slabs subjected to low-velocity drop impact loading. *Front. Mater.* 9. Article in press. doi:10.3389/fmats.2022.1061297

Andreão, P. V., Suleiman, A. R., Cordeiro, G. C., and Nehdi, M. L. (2020). Beneficiation of sugarcane bagasse ash: Pozzolanic activity and leaching behavior. *Waste Biomass Valor* 11, 4393–4402.

Andreão, P. V., Suleiman, A. R., Cordeiro, G. C., and Nehdi, M. L. (2019). Sustainable use of sugarcane bagasse ash in cement-based materials. *Green Mater* 7, 61–70. doi:10.1680/jgrma.18.00016

Anjos, M. A. S., Araújo, T. R., Ferreira, R. L. S., Farias, E. C., and Martinelli, A. E. (2020). Properties of self-leveling mortars incorporating a high-volume of sugar cane bagasse ash as partial Portland cement replacement. *J. Build. Eng.* 32, 101694. doi:10.1016/j.jobe.2020.101694

ASTM C1585-13 (2013). *Standard test method for measurement of rate of absorption of water by hydraulic cement concretes*. West Conshohocken, PA, USA: ASTM. doi:10.1520/C1585-13.2

ASTM C39 (2016). *ASTM standard C39/C39m-16, standard test method for compressive strength of cylindrical concrete specimens*. West Conshohocken, PA, USA: ASTM.

ASTM C618-17a (2017). *Standard specification for coal fly ash and raw or calcined natural pozzolan for use in concrete*. West Conshohocken, PA, USA: ASTM, 1–5.

ASTM C78 (2016). *Standard test method for flexural strength of concrete*. West Conshohocken, PA, USA: ASTM.

ASTM D1557 (2021). *Standard test methods for laboratory compaction characteristics of soil using modiefied effort (56,000 Ft-lbf/ft3 (2,700 kN-m/m3))*, 3. West Conshohocken, PA, USA: ASTM, 1–10.

ASTM Standards C-293 (2002). *Standard test method for flexural strength of concrete (using simple beam with center-point loading)*. West Conshohocken, PA, USA: ASTM.

Bahurudeen, A., Kanraj, D., Gokul Dev, V., and Santhanam, M. (2015). Performance evaluation of sugarcane bagasse ash blended cement in concrete. *Cem. Concr. Compos.* 59, 77–88. doi:10.1016/j.cemconcomp.2015.03.004

Bahurudeen, A., and Santhanam, M. (2015). Influence of different processing methods on the pozzolanic performance of sugarcane bagasse ash. *Cem. Concr. Compos.* 56, 32–45. doi:10.1016/j.cemconcomp.2014.11.002

Bartošek, J. (2014). Czech cane sugar factories II. *List. Cukrov. Repar.* 130, 328–334.

Bentz, D. P., Ferraris, C. F., Jones, S. Z., Lootens, D., and Zunino, F. (2017). Limestone and silica powder replacements for cement: Early-age performance. *Cem. Concr. Compos.* 78, 43–56. doi:10.1016/j.cemconcomp.2017.01.001

BIS:383 (1970). *Specification for coarse and fine aggregates from natural sources for concrete*. New Delhi, India: Indian Standard, 1–24.

Cetin, E., Moghtaderi, B., Gupta, R., and Wall, T. F. (2004). Influence of pyrolysis conditions on the structure and gasification reactivity of biomass chars. *Fuel* 83, 2139–2150. doi:10.1016/j.fuel.2004.05.008

Channa, S. H., Mangi, S. A., Bheel, N., Soomro, F. A., and Khahro, S. H. (2022). Short-term analysis on the combined use of sugarcane bagasse ash and rice husk ash as supplementary cementitious material in concrete production. *Environ. Sci. Pollut. Res.* 29, 3555–3564. doi:10.1007/s11356-021-15877-0

Chusilp, N., Jaturapitakkul, C., and Kiattikomol, K. (2009). Effects of LOI of ground bagasse ash on the compressive strength and sulfate resistance of mortars. *Constr. Build. Mater.* 23, 3523–3531. doi:10.1016/j.conbuildmat.2009.06.046

Cordeiro, G. C., Filho, R. D. T., and De Almeida, R. S. (2011). Influence of ultrafine wet grinding on pozzolanic activity of submicrometre sugar cane bagasse ash. *Adv. Appl. Ceram.* 110, 453–456. doi:10.1179/1743676111Y.0000000050

Cordeiro, G. C., and Kurtis, K. E. (2017). Effect of mechanical processing on sugar cane bagasse ash pozzolanicity. *Cem. Concr. Res.* 97, 41–49. doi:10.1016/j.cemconres.2017.03.008

Cordeiro, G. C., Paiva, O. A., Toledo Filho, R. D., Fairbairn, E. M. R., and Tavares, L. M. (2018). Long-term compressive behavior of concretes with sugarcane bagasse ash as a supplementary cementitious material. *J. Test. Eval.* 46, 20160316–20160573. doi:10.1520/JTE20160316

Cordeiro, G. C., Tavares, L. M., and Toledo Filho, R. D. (2016). Improved pozzolanic activity of sugar cane bagasse ash by selective grinding and classification. *Cem. Concr. Res.* 89, 269–275. doi:10.1016/j.cemconres.2016.08.020

Cordeiro, G. C., Toledo Filho, R. D., Tavares, L. M., and Fairbairn, E. D. M. R. (2009). Ultrafine grinding of sugar cane bagasse ash for application as pozzolanic admixture in concrete. *Cem. Concr. Res.* 39, 110–115. doi:10.1016/j.cemconres.2008.11.005

Deepika, S., Anand, G., Bahurudeen, A., and Santhanam, M. (2017). Construction products with sugarcane bagasse ash binder. *J. Mater. Civ. Eng.* 29, 04017189. doi:10.1061/(asce)mt.1943-5533.0001999

Duxson, P., Lukey, G. C., and van Deventer, J. S. J. (2006). Thermal evolution of metakaolin geopolymers: Part 1—physical evolution. *J. Non. Cryst. Solids* 352, 5541–5555. doi:10.1016/j.jnoncrysol.2006.09.019

Frías, M., Villar, E., and Savastano, H. (2011). Brazilian sugar cane bagasse ashes from the cogeneration industry as active pozzolans for cement manufacture. *Cem. Concr. Compos.* 33, 490–496. doi:10.1016/j.cemconcomp.2011.02.003

Ganesan, K., Rajagopal, K., and Thangavel, K. (2007). Evaluation of bagasse ash as supplementary cementitious material. *Cem. Concr. Compos.* 29, 515–524. doi:10.1016/j.cemconcomp.2007.03.001

Horvath, J. S. (1998). *The compressible-inclusion function of EPS geofoam: Analysis and design methodologies; research report No. CE/GE-98-1; manhattan college*. Bronx, NY, USA: Civil Engineering Department. doi:10.13140/RG.2.2.26209.35685

Iman, M., Mortazavi, S. J., Manfredi, M., Awoyera, P. O., Mansouri, E., Khaki, A., et al. (2023). Development of new material models for thermal behavior of cold-formed G-450 and G-550 steels in OpenSees software. *J. Archit. Eng.* 29 (2). doi:10.1061/JAEIED.AEENG-1491

Khan, M. A., El Rimawi, J. A., and Silberschmidt, V. (2017). Numerical representation of multiple premature failures in steel-plated RC beams. *Int. J. Comput. Methods* 14 (4), 1750035. doi:10.1142/S0219876217500359

Khan, M. A., and El Rimawi, J. A. (Forthcoming). "On peeling-versus-shear failures in prematurely collapsing RC beams strengthened in flexure," in *Practice periodical on structural design and construction*. (ASCE). doi:10.1061/PPSCFX/SCENG-1224

Khan, M., and Ali, M. (2019). Improvement in concrete behavior with fly ash, silica-fume and coconut fibres. *Constr. Build. Mater.* 203, 174–187. doi:10.1016/j.conbuildmat.2019.01.103

Khan, M., and Ali, M. (2016). Use of glass and nylon fibers in concrete for controlling early age micro cracking in bridge decks. *Constr. Build. Mater.* 125, 800–808. doi:10.1016/j.conbuildmat.2016.08.111

Khan, M., Cao, M., and Ali, M. (2018). Effect of basalt fibers on mechanical properties of calcium carbonate whisker-steel fiber reinforced concrete. *Constr. Build. Mater.* 192, 742–753. doi:10.1016/j.conbuildmat.2018.10.159

Khan, M., Lao, J., and Dai, J-G. (2022). Comparative study of advanced computational techniques for estimating the compressive strength of UHPC. *J. Asian Concr. Fed.* 8 (1), 51–68. doi:10.18702/acf.2022.6.8.1.51

Khan, M. A. (2022). Bond parameters for peeling and debonding in thin plated RC beams subjected to mixed mode loading – framework. *Adv. Struct. Eng.* 25 (3), 662–682. doi:10.1177/13694332211065184

Khan, M. A., El Rimawi, J., and Silberschmidt, V. (2017). Relative behaviour of premature failures in adhesively plated RC beam using controllable and existing parameters. *J. Compos. Struct.* 180, 75–87. doi:10.1016/j.compstruct.2017.08.006

Khan, M. A., Imam, M. K., Irshad, K., Ali, H. M., Hasan, M. A., and Islam, S. (2021). Comparative overview of the performance of cementitious and non-cementitious nanomaterials in mortar at normal and elevated temperatures. *Nanomaterials* 11 (4), 911. doi:10.3390/nano11040911

Khan, M. A., Silberschmidt, V., and El Rimawi, J. (2017). Controlled failure warning and mitigation of prematurely failing beam through adhesive. *J. Compos. Struct.* 161, 119–131. doi:10.1016/j.compstruct.2016.11.049

Khan, M. A. (2021). Toward key research gaps in design recommendations on flexurally plated RC beams susceptible to premature failures. *J. Bridge Eng.* 26, 9. doi:10.1061/(ASCE)BE.1943-5592.0001772

Khan, M. A. (2021). Towards progressive debonding in composite RC beams subjected to thermo-mechanical bending with boundary constraints – a new analytical solution. *J. Compos. Struct.* 274, 114334. doi:10.1016/j.compstruct.2021.114334

Khawaja, S. A., Javed, U., Zafar, T., Riaz, M., Zafar, M. S., and Khan, M. K. (2021). Eco-friendly incorporation of sugarcane bagasse ash as partial replacement of sand in foam concrete. *Clean. Eng. Technol.* 4, 100164. doi:10.1016/j.clet.2021.100164

Kirschner, A. V., and Harmuth, H. (2004). Investigation of geopolymer binders with respect to their application for building materials. *Ceram. Silik.* 48, 117–120.

Kuruba, E. K., Rao, P. V. K. J., Khokhar, D., and Patel, S. (2020). Technologies for preparation of solid and granular jaggery: A review. *Curr. J. Appl. Sci. Technol.* 39, 105–113. doi:10.9734/cjast/2020/v39i3030978

Landa-Ruiz, L., Landa-Gómez, A., Mendoza-Rangel, J. M., Landa-Sánchez, A., Ariza-Figueroa, H., Méndez-Ramírez, C. T., et al. (2021). Physical, mechanical and durability properties of ecofriendly ternary concrete made with sugar cane bagasse ash and silica fume. *Crystals* 11 (9), 1012. doi:10.3390/cryst11091012

Le, D. H., Sheen, Y. N., and Lam, M. N. T. (2018). Fresh and hardened properties of self-compacting concrete with sugarcane bagasse ash–slag blended cement. *Constr. Build. Mater.* 185, 138–147. doi:10.1016/j.conbuildmat.2018.07.029

Liu, H. L., Deng, A., and Chu, J. (2006). Effect of different mixing ratios of polystyrene pre-puff beads and cement on the mechanical behaviour of lightweight fill. *Geotext. Geomembr.* 24, 331–338. doi:10.1016/j.geotexmem.2006.05.002

Mandal, D., Ram Rathan Lal, B., and Shankar, K. (2018). "Compressive strength behaviour of glass fibre reinforced blast furnace slag-based material," in Proceedings of the 11th International Conference on Geosynthetics, Seoul, Korea, 16–21 September 2018, 1874–1880.

Mangi, S. A., Memon, Z. A., Khahro, S. H., Memon, R. A., and Memon, A. H. (2020). Potentiality of industrial waste as supplementary cementitious material in concrete production. *Int. Rev. Civ. Eng.* 11, 214–221. doi:10.15866/irece.v11i5.18779

Mansouri, E., Manfredi, M., and Hu, J-W. (2022). Environmentally friendly concrete compressive strength prediction using hybrid machine learning. *Sustainability* 14 (20), 12990. doi:10.3390/su142012990

Maroliya, M. K. (2012). A qualitative study of reactive powder concrete using X-ray diffraction technique. *IOSR J. Eng.* 2, 12–16. doi:10.9790/3021-02911216

Martirena, F., and Monzó, J. (2018). Vegetable ashes as supplementary cementitious materials. *Cem. Concr. Res.* 114, 57–64. doi:10.1016/j.cemconres.2017.08.015

Matsuda, H., Shinozaki, H., Ishikura, R., and Kitayama, N. (2008). "Application of granulated blast furnace slag to the earthquake resistant Earth structure as a geo-material," in *Proceedings of the 14th world conference on earthquake engineering beijing* China.

Memon, S. A., Javed, U., Shah, M. I., and Hanif, A. (2022). Use of processed sugarcane bagasse ash in concrete as partial replacement of cement: Mechanical and durability properties. *Buildings* 12 (10), 1769. doi:10.3390/buildings12101769

Mugahed, A., Shan-Shan, H., Onaizi, A. M., Murali, G., and Abdelgader, H. S. (2022). Fire spalling behavior of high-strength concrete: A critical review. *Constr. Build. Mater.* 341, 127902. doi:10.1016/j.conbuildmat.2022.127902

Najm, H. M., and Ahmad, S. (2022). The use of waste ceramic optimal concrete for A cleaner and sustainable environment—a case study of mechanical properties. *Civ. Environ. Eng. Rep.* 32, 85–115. doi:10.2478/ceer-2022-0030

Najm, H. M., Nanayakkara, O., Ahmad, M., and Sabri Sabri, M. M. (2022). Mechanical properties, crack width, and propagation of waste ceramic concrete subjected to elevated temperatures: A comprehensive study. *Materials* 15, 2371. doi:10.3390/ma15072371

Najm, H. M., Nanayakkara, O., and Sabri, M. M. S. (2022). Destructive and non-destructive evaluation of fibre-reinforced concrete: A comprehensive study of mechanical properties. *Materials* 15, 4432. doi:10.3390/ma15134432

Nanayakkara, O., Najm, H. M., and Sabri, M. M. S. (2022). Effect of using steel bar reinforcement on concrete quality by ultrasonic pulse velocity measurements. *Materials* 15, 4565. doi:10.3390/ma15134565

Nikhade, H. R., and Lal, B. (2021). Experimental studies on sugar cane bagasse ash based geomaterials. *Int. J. Eng. Manag. Res.* 11, 1–3. doi:10.31033/ijemr.11.5.1

Nikhade, H. R., and Lal, B. (2023). "Studies on sugar cane bagasse ash and blast furnace slag-based geomaterial," in *Indian geotechnical and geoenvironmental engineering conference* (Singapore: Springer), 25–32.

Osei, D. Y., Mustapha, Z., and Zebilila, M. D. (2020). Compressive strength of concrete using different curing methods. *J. Soc. Dev. Sci.* 10, 30–38. doi:10.22610/jsds.v10i3(s).2983

Prabhath, N., Kumara, B. S., Vithanage, V., Samarathunga, A. I., Sewwandi, N., Maduwantha, K., et al. (2022). A review on the optimization of the mechanical properties of sugarcane-bagasse-ash-integrated concretes. *J. Compos. Sci.* 6 (10), 283. doi:10.3390/jcs6100283

Qaidi, S. M. A., Tayeh, B. A., Isleem, H. F., AzevedoAfonso, R. G. D., Unis, H. A., et al. (2022). Sustainable utilization of red mud waste (bauxite residue) and slag for the production of geopolymer composites: A review. *Case Stud. Constr. Mater.* 16, e00994. doi:10.1016/j.cscm.2022.e00994

Rajasekar, A., Arunachalam, K., Kottaisamy, M., and Saraswathy, V. (2018). Durability characteristics of ultra high strength concrete with treated sugarcane bagasse ash. *Constr. Build. Mater.* 171, 350–356. doi:10.1016/j.conbuildmat.2018.03.140

Rakhimova, N. R., and Rakhimov, R. Z. (2014). A review on alkali-activated slag cements incorporated with supplementary materials. *J. Sustain. Cem. Mater.* 3, 61–74. doi:10.1080/21650373.2013.876944

Ram Rathan Lal, B., and Badwaik, V. N. (2016). Experimental studies on bottom ash and expanded polystyrene beads–based geomaterial. *J. Hazard. Toxic, Radioact. Waste* 20 (2), 04015020. doi:10.1061/(asce)hz.2153-5515.0000305

Ram Rathan Lal, B., and Nawkhare, S. S. (2016). Experimental study on plastic strips and EPS beads reinforced bottom ash based material. *Int. J. Geosynth. Ground Eng.* 2 (3), 25–12. doi:10.1007/s40891-016-0066-2

Rao, M. S. C., Vijayalakshmi, M. M., and Praveenkumar, T. R. (2021). Behaviour of green concrete (blended concrete) using agro-industrial waste as partial replacement of cement along with nanoparticles. *Appl. Nanosci.* 1, 1–9. doi:10.1007/s13204-021-01917-1

Rodrigues, J. A. R. (2011). Do engenho à biorrefinaria: A usina de açúcar como empreendimento industrial para a geração de produtos bioquímicos e biocombustíveis. *Quim. Nova* 34, 1242–1254. doi:10.1590/S0100-40422011000700024

Rodríguez de Sensale, G., and Rodríguez Viacava, I. (2018). A study on blended Portland cements containing residual rice husk ash and limestone filler. *Constr. Build. Mater.* 166, 873–888. doi:10.1016/j.conbuildmat.2018.01.113

Rubenstein, M. (2012). Emissions from the cement industry. *State Planet* 11, 1–9.

Saleh, H. M., Salman, A. A., Faheim, A. A., and El-Sayed, A. M. (2020). Sustainable composite of improved lightweight concrete from cement kiln dust with grated poly(styrene). *J. Clean. Prod.* 277, 123491. doi:10.1016/j.jclepro.2020.123491

Setayesh Gar, P., Suresh, N., and BindiganavileSugar, V. (2017). Sugar cane bagasse ash as a pozzolanic admixture in concrete for resistance to sustained elevated temperatures. *Constr. Build. Mater.* 153, 929–936. doi:10.1016/j.conbuildmat.2017.07.107

Singh, N. B., Singh, V. D., and Rai, S. (2000). Hydration of bagasse ash-blended Portland cement. *Cem. Concr. Res.* 30, 1485–1488. doi:10.1016/S0008-8846(00)00324-0

Stafford, F. N., Raupp-Pereira, F., Labrincha, J. A., and Hotza, D. (2016). Life cycle assessment of the production of cement: A Brazilian case study. *J. Clean. Prod.* 137, 1293–1299. doi:10.1016/j.jclepro.2016.07.050

Talero, R., Rahhal, V., Potapov, V. V., Serdan, A. A., Kashpura, V. N., Gorbach, V. A., et al. (2007). AN2521 application note:19 V–75 W laptop adapter with tracking boost PFC pre-regulator, using the L6563 and L6668. *Constr. Build. Mater.* 1, 2–6.

Thomas, R. J., Lezama, D., and Peethamparan, S. (2017). On drying shrinkage in alkali-activated concrete: Improving dimensional stability by aging or heat-curing. *Cem. Concr. Res.* 91, 13–23. doi:10.1016/j.cemconres.2016.10.003

van Deventer, J. S. J., Nicolas, R. S., Ismail, I., Bernal, S. A., Brice, D. G., and Provis, J. L. (2014). Microstructure and durability of alkali-activated materials as key parameters for standardization. *J. Sustain. Cem. Mater.* 4, 116–128. doi:10.1080/21650373.2014.979265

Wen, C., Zhang, P., Wang, J., and Hu, S. (2022). Influence of fibers on the mechanical properties and durability of ultra-high-performance concrete: A review. *J. Build. Eng.* 52 (2022), 104370. doi:10.1016/j.jobe.2022.104370

Xu, Q., Ji, T., Gao, S. J., Yang, Z., and Wu, N. (2018). Characteristics and applications of sugar cane bagasse ash waste in cementitious materials. *Materials* 12, 39. doi:10.3390/ma12010039

Yashwanth, M. K., Avinash, G. B., Raghavendra, A., and Kumar, B. G. N. (2017). An experimental study on alternative cementitious materials: Bagasse ash as partial replacement for cement in structural lightweight concrete. *Indian Concr. J.* 91, 51–58.

Zareei, S. A., Ameri, F., and Bahrami, N. (2018). Microstructure, strength, and durability of eco-friendly concretes containing sugarcane bagasse ash. *Constr. Build. Mater.* 184, 258–268. doi:10.1016/j.conbuildmat.2018.06.153

Zhang, P., Gao, Z., Wang, J., Guo, J., and Wang, I. (2022). Influencing factors analysis and optimized prediction model for rheology and flowability of nano-SiO2 and PVA fiber reinforced alkali-activated composites. *J. Clean. Prod.* 366 (2022), 132988. doi:10.1016/j.jclepro.2022.132988

Zhang, P., Han, X., Hu, S., Wang, J., and Wang, T. (2022). High-temperature behavior of polyvinyl alcohol fiber-reinforced metakaolin/fly ash-based geopolymer mortar. *Compos. Part B Eng.* 244 (2022), 110171. doi:10.1016/j.compositesb.2022.110171

Zhang, P., Peng, Y., Guan, J., and Guo, J. (2022). Fracture behavior of multi-scale nano-SiO2 and polyvinyl alcohol fiber reinforced cementitious composites under the complex environments. *Theor. Appl. Fract. Mech.* 122 (2022), 103584. doi:10.1016/j.tafmec.2022.103584

Zhang, P., Zhang, P., Wu, J., Zhang, Y., and Guo, J. (2022). Mechanical properties of polyvinyl alcohol fiber-reinforced cementitious composites after high-temperature exposure. *Gels* 8 (10), 662. doi:10.3390/gels8100662